The Accumulation of Antifreeze Proteins on Ice is Determined by Adsorption

Aniket U. Thosar[1], Yitzhar Shalom[2,3], Ido Braslavsky[4], Ran Drori[2,3], Amish J. Patel[1*]*

[1]Department of Chemical and Biomolecular Engineering, University of Pennsylvania, Philadelphia, PA 19104, USA.

[2]Department of Chemistry and Biochemistry, Yeshiva University, New York, NY 10016, USA.

[3]Department of Physics, Katz School of Science and Health, Yeshiva University, New York, NY 10016, USA.

[4]The Robert H. Smith Faculty of Agriculture, Food and Environment, Institute of Biochemistry, Food Science and Nutrition, The Hebrew University of Jerusalem, Rehovot 7610001, Israel.

Keywords: AFPs, Binding, Diffusion, Thermal Hysteresis

Abstract

Antifreeze proteins (AFPs) facilitate the survival of diverse organisms in frigid environments by adsorbing to ice crystals and suppressing their growth. The rate of AFP accumulation on ice is determined by an interplay between AFP diffusion from the bulk solution to the ice-water interface and the subsequent adsorption of AFPs to the interface. To interrogate the relative importance of these two processes, here we combine non-equilibrium fluorescence experiments with a reaction-diffusion model. We find that as diverse AFPs accumulate on ice, their concentration in the aqueous solution does not develop a gradient but remains equal to its bulk concentration throughout our experiments. These findings lead us to conclude that AFP accumulation on ice crystals, which are smaller than 100 microns in radius, is not limited by the diffusion of AFPs, but by the kinetics of AFP adsorption. Our results imply that mass transport limitations do not hinder AFPs from performing their biological function.

INTRODUCTION

A wide variety of organisms, such as fish, insects, fungi, bacteria and plants, which live in sub-freezing temperatures, have evolved a unique class of biomolecules known as antifreeze proteins (AFPs) which facilitate the survival of their host organisms by suppressing ice growth in their cells and body fluids[1,2]. Optical microscopy experiments using aqueous solutions of fluorescently-tagged AFPs have shown that for AFPs to function, they must adsorb to ice crystals and accumulate at the ice-water interface[3–10]. At low supercooling, i.e., close to the melting temperature of the crystal, T_{m}, small surface AFP fractions are sufficient to arrest ice growth; however, as the supercooling ($\Delta T = T_{\mathrm{m}} - T$) is increased, adsorbed AFPs are eventually engulfed by ice, resulting in a burst of sudden ice growth[11] at a critical supercooling, ΔT^*. The supercooling, ΔT^*, represents the range of temperatures over which an AFP suppress the growth of ice crystals, and is known as the thermal hysteresis activity of the AFP[12,13].

Theory, molecular simulations and experiments have all shown that ΔT^* increases with the surface concentration, n, of AFPs adsorbed to the ice-water interface[3,5,14,15]; at higher surface concentrations, AFPs are more effective at resisting engulfment by ice. Therefore, ΔT^* depends on the rate at which AFPs accumulate on the ice crystal[4,16], which in turn, is determined by an interplay between the diffusion of AFPs from bulk water to the ice-water interface and their subsequent adsorption to the interface (Figure 1a). Thus, the relative rates of AFP diffusion and adsorption, and whether one of these processes is rate-limiting, dictates not just the surface AFP concentration, n (and therefore the ΔT^*), but also how n depends on quantities, such as the size and shape of the AFP, the viscosity of the solution, and the radius of the ice crystal.

Molecular simulations of the hyperactive antifreeze protein, *Tm*AFP, using the mW water model[17] suggest that AFP binding to ice is fast and occurs over timescales of tens of nanoseconds. Assuming that the intrinsic kinetics of AFP-ice binding are fast, Kamat *et al.*[18,19] elucidated how the overall rate of AFP adsorption is influenced by the restricted orientational relaxation of rod-like AFP molecules as they approach the ice surface, and concluded that for micron-sized ice crystals, rates of diffusion and adsorption become comparable. In contrast, in analyzing their fluorescence experiments, Drori and co-workers assumed that the accumulation of AFPs was determined by the intrinsic kinetics of adsorption[3,4,8]. However, a definitive determination of whether the accumulation of AFPs at the ice-water interface is limited by diffusion or adsorption remains elusive.

To uncover the relative importance of AFP diffusion and adsorption in determining the accumulation of AFPs on ice, here we employ non-equilibrium fluorescence experiments, which enable us to obtain the spatial variation of AFP concentration away from the ice-water interface and its evolution with time. By using a reaction-diffusion model to analyze the process, we show that when AFP accumulation is diffusion-limited, AFP concentration near the ice-water interface must be depleted relative to the bulk, whereas when AFP accumulation is limited by adsorption, no gradients in AFP concentration are expected. By characterizing the spatial concentration profiles for a variety of AFPs near ice crystals that are roughly 10 microns in radius, we find that AFP concentration is not depleted near the ice-water interface. Our results suggest that AFP diffusion is fast relative to adsorption and that the accumulation of diverse AFPs on ice crystals that are smaller than 100 microns in radius is limited by the kinetics of adsorption.

RESULTS and DISCUSSION

To characterize the kinetics of AFP accumulation on ice, we performed non-equilibrium experiments using a wide variety of fluorescently tagged AFPs. As described in detail previously[3,4], a single ice crystal was grown from the AFP solution of interest by first freezing the entire sample and slowly melting the bulk ice to obtain a single crystal. To study different AFP concentrations, the above process was repeated. The temperature was then raised by roughly 0.01 °C above T_m for a few seconds to melt the ice crystal and achieve an AFP-free ice-water interface. After the ice-water interface retreated by 3-5 μm and no fluorescence intensity was observed at the interface, the temperature was lowered by roughly 0.02 - 0.03 °C until crystal melting ceased. At this point, the AFPs in solution started to accumulate at the ice-water interface; this point was considered to be the start of our experiment (i.e., $t = 0$), and the fluorescence intensity across the ice-water interface was then recorded for up to 2000 seconds. Additional experimental details are included in the SI.

In Figure 1, spatiotemporal fluorescence intensity profiles are shown for the 4.1 μM QAE isoform of AFPIII tagged with a green fluorescence protein (GFP)[20]. At the start of the experiment, the fluorescence intensity across the prism plane of the ice crystal was found to vary in a sigmoidal manner over a distance of roughly a micron. We note that although intrinsic width of ice-water interface is expected to be in nanometers, the precise location of the ice-water interface varies across the illuminated region, giving rise to a variation in our intensity profiles over a few microns.

As AFPIII molecules adsorb to, and accumulate at, the ice-water interface, the fluorescence intensity displays a peak in the interfacial region that grows with time.

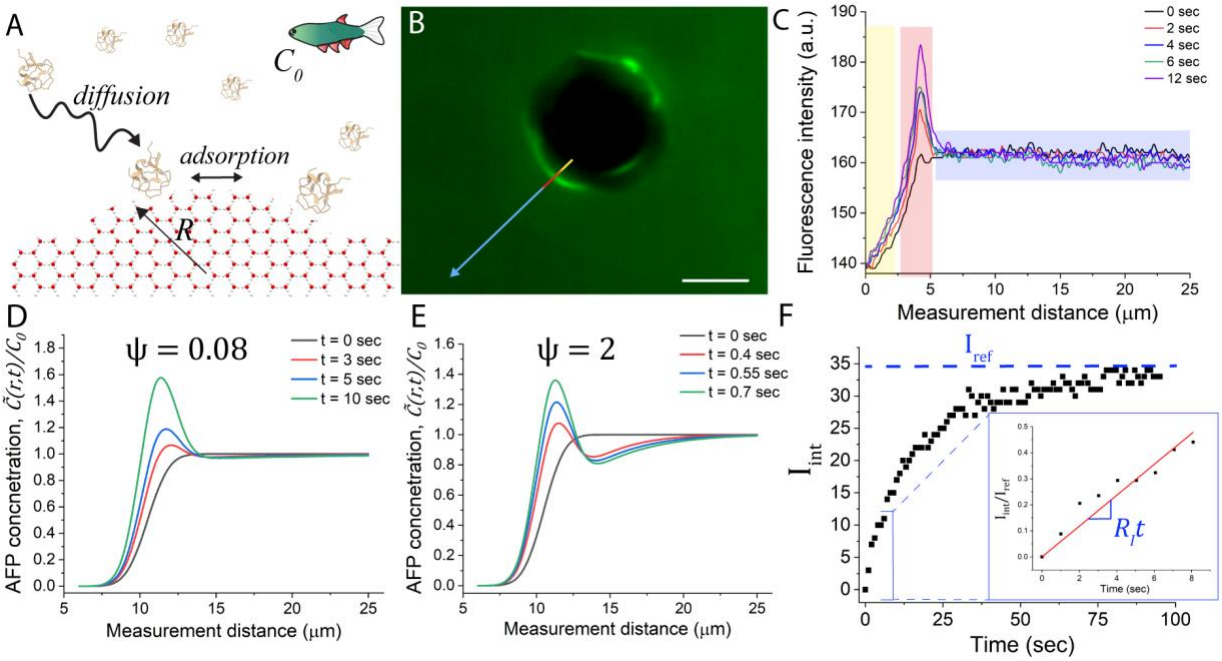

Figure 1. (A) To accumulate on an ice crystal, AFPs must diffuse through bulk water and adsorb to the ice-water interface. (B) Optical micrograph highlighting the accumulation of fluorescently labeled AFPs on the surface of an ice crystal (center, dark). As depicted by the arrow, fluorescence intensity was measured across the ice-water interface and into the 4.1 μM AFPIII-QAE solution. Scale bar = 10 μm. (C) The evolution of the radial fluorescence intensity profile with time is shown, with regions corresponding to bulk ice (yellow), the interface (red) and the aqueous solution (blue) being highlighted. (D, E) Normalized AFP concentration profiles, $\tilde{C}(r,t)/C_0$, for small (D) and large (E) values of the dimensionless number, ψ. For $\psi < 1$ (slow adsorption), AFP concentration remains equal to its bulk value everywhere in solution, whereas for $\psi > 1$ (slow diffusion), AFP concentration drops substantially near ice-water interface within 1 s and recovers to its bulk value more than 10 microns away from the interface. (F) The fluorescence intensity, I_{int}, due to the adsorbed AFPs, is shown as a function of time, and its steady-state value, I_{ref}, is highlighted. The inset focuses on $I_{\mathrm{int}}/I_{\mathrm{ref}}$ at early times (i.e., for low surface coverage), and a linear fit (red) to the data is used to obtain the initial rate, $\mathcal{R}_I$, of increase of $I_{\mathrm{int}}/I_{\mathrm{ref}}$.

To better understand the spatiotemporal fluorescence intensity profiles shown in Figure 1, and their implications for the relative rates of AFP diffusion and adsorption, we employ a reaction-diffusion model to describe the accumulation of AFPs onto a spherical ice crystal of radius R. The AFP concentration, $C(r,t)$, at a distance r from the center of the ice crystal at any time t must follow the transient diffusion equation:

$$\frac{\partial C}{\partial t} = \frac{D}{r^2}\frac{\partial}{\partial r}\left(r^2\frac{\partial C}{\partial r}\right), \tag{1}$$

where D is the diffusion coefficient of AFPs in water. At the start of our non-equilibrium experiment, the AFP concentration profile obeys the initial condition that $C(r > R, t = 0) = C_0$, where C_0 is the bulk AFP concentration in solution. The AFP concentration profile must also obey the boundary conditions that: (i) far from the ice crystal, the AFP concentration approaches its bulk value, i.e., as $r \to \infty$, $C = C_0$; and that: (ii) at the ice-water interface, the diffusive AFP flux is matched by the net rate of AFP adsorption per unit interfacial area, $\mathcal{R}_{\mathrm{ads}}$, i.e.,

$$\text{at } r = R, \quad D\frac{\partial C}{\partial r} = \mathcal{R}_{\mathrm{ads}} \equiv \frac{\partial n}{\partial t} = k_{\mathrm{on}}\, C(n_{\mathrm{sat}} - n) - k_{\mathrm{off}}\, n, \tag{2}$$

where adsorption and desorption are assumed to obey Langmuir kinetics with the corresponding rate constants, k_{on} and k_{off}, encompassing both AFP orientation and binding; $n_{\mathrm{sat}} = L_{\mathrm{sat}}^{-2}/N_{\mathrm{Avo}}$ is the surface concentration of AFPs when the ice-water interface is saturated, L_{sat} is corresponding separation between bound AFPs, and N_{Avo} is Avogadro's number.

When AFP surface coverage, $\theta \equiv n/n_{\mathrm{sat}}$, is small, the net adsorption flux can be approximated to be independent of n, i.e., $\mathcal{R}_{\mathrm{ads}} \approx k_{\mathrm{on}}\, n_{\mathrm{sat}}\, C$. In fact, as shown by Miura and Seki[21], such an approximation is reasonable until $\theta \approx 0.4$. Under this approximation, the solution to the spatiotemporal AFP concentration profile, $C(r, t)$, is independent of the precise form of adsorption/desorption kinetics (i.e., the dependence of $\mathcal{R}_{\mathrm{ads}}$ on n), and is given by:

$$\frac{C(\hat{r},\hat{t})}{C_0} = 1 - \left(\frac{\psi}{\hat{r}+1+\psi}\right)\left[\mathrm{erfc}\left(\frac{\hat{r}}{2\sqrt{\hat{t}}}\right) - \mathrm{e}^{\hat{r}+\hat{t}}\,\mathrm{erfc}\left(\frac{\hat{r}}{2\sqrt{\hat{t}}} + \sqrt{\hat{t}}\right)\right], \tag{3}$$

where $\psi = (k_{\mathrm{on}}n_{\mathrm{sat}})/(D/R)$ is a dimensionless number that quantifies the relative rates of AFP adsorption and diffusion (akin to a Damköhler number), $\hat{r} \equiv (1+\psi)(r-R)/R$ is a dimensionless

radial coordinate, $\hat{t} \equiv t/\tau_{\mathrm{tr}}$ is a dimensionless time, $\tau_{\mathrm{tr}} \equiv \tau_{\mathrm{diff}}/(1+\psi)^2$ is the transient time required for the development of concentration gradients, and $\tau_{\mathrm{diff}} \equiv R^2/D$ is the characteristic time for AFP diffusion. The corresponding rate of accumulation of bound AFPs per unit ice-water interfacial area can be obtained from the diffusive flux at the interface as:

$$\frac{\partial n}{\partial t} = D\,\frac{\partial C}{\partial r}\Big|_{r=R} = \frac{DC_0}{R}\left(\frac{\psi}{1+\psi}\right)\left[1+\psi\,\mathrm{e}^{\hat{t}}\ \mathrm{erfc}\left(\sqrt{\hat{t}}\right)\right] \qquad (4)$$

The AFP surface concentration, $n(t)$, can then be obtained by integrating Equation 4 from the initial condition, $n(t=0)=0$. To account for the dispersion of the ice-water interface in our experiments, we convolute the AFP concentration (both in solution and at the interface) using a Gaussian smearing function, $G(r;\sigma) = e^{-r^2/2\sigma^2}/\sqrt{2\pi\sigma^2}$, with a width, $\sigma = 1$ μm, according to:

$$\tilde{C}(r,t) = \int_{-\infty}^{\infty} G(r-r';\sigma)\,[C(r',t) + n(t)\delta(r'-R)]\,dr'. \qquad (5)$$

To interpret our experiments using the theoretical framework laid out in Equations 3 – 5, we note that the typical radius of our ice crystals is roughly $R = 10$ μm, and use the Stokes-Einstein relationship, $D = \frac{k_{\mathrm{B}}T_{\mathrm{m}}}{6\pi\eta R_{\mathrm{AFP}}}$, to estimate the diffusion coefficient of AFPs in water; k_{B} is Boltzmann's constant, η is the viscosity of water, and R_{AFP} is the hydrodynamic radius of AFP. We note that at strong supercooling, as water approaches its glass transition temperature, its viscosity increases sharply, and the Stokes-Einstein relationship breaks down; however, for temperatures pertinent to AFP function (up to 5 K below T_{m}), deviations of less than 10% from the Stokes-Einstein relationship are expected and η increases by less than 15% relative to T_{m} [22]. Assuming R_{AFP} to be 3 nm for our GFP-tagged AFPs[7], and noting that $\eta(T_{\mathrm{m}}) \approx 1.8$ cP, we estimate D to be roughly 3.3×10^{-11} m$^2/s$. In contrast, obtaining an estimate of the intrinsic adsorption rate coefficient, k_{on} (and correspondingly of ψ), is not straightforward. By combining

our experimental measurements with the theoretical framework described above, we now seek to uncover whether AFP accumulation at the ice-water interface is limited by slow adsorption kinetics ($\psi \ll 1$) or by slow diffusion ($\psi \gg 1$).

To this end, we first consider the limiting cases of adsorption kinetics being slow relative to diffusion (low k_{on} and $\psi \ll 1$) and that of adsorption being fast (high k_{on} and $\psi \gg 1$). The corresponding smeared concentration profiles, $\tilde{C}(r,t)$, which correspond closely to the experimentally measured fluorescent intensities, are shown in Figures 1D and 1E. In both cases, $\tilde{C}(r,t)$ displays a peak at the ice-water interface, which grows with time as AFPs adsorb to, and accumulate at, the interface. When the intrinsic kinetics of adsorption are slower than the diffusive flux, i.e., $\psi \ll 1$, diffusion rapidly replaces AFPs that adsorb to the ice-water interface, resulting in $\tilde{C}(r,t) \approx C_0$ away from the interfacial region, i.e., AFP concentration is equal to its bulk value everywhere in the solution (Figure 1D). In contrast, when AFP adsorption kinetics are faster than their diffusive supply, i.e., when $\psi > 1$, the solution concentration, $\tilde{C}(r,t)$, drops below C_0 with the decrease being most pronounced closest to ice-water interface (Figure 1E).

In particular, as described in detail in the SI, the solution AFP concentration adjacent to the ice-water interface, $C(R,t) \equiv C_{\mathrm{surf}}$, decreases asymptotically to $C_0/(1+\psi)$ over a transient timescale, $\tau_{\mathrm{tr}} = \tau_{\mathrm{diff}}/(1+\psi)^2$, where $\tau_{\mathrm{diff}} = R^2/D$ is roughly equal to 3 s for our experiments. For $\psi \gg 1$, we thus expect C_{surf} to decrease from its initial value of C_0 to a small fraction of C_0 over a transient time of a fraction of a second. Moreover, the length scale over which $C(r,t)$ varies from its interfacial value, C_{surf}, to its bulk value, C_0, grows as $\sqrt{Dt}$ and is expected to be roughly $2R/(1+\psi)$ at $t = \tau_{\mathrm{tr}}$. We note that when the concentration profiles are smeared, the signals from the depletion of the AFPs in the solution (near the interface) and from their accumulation at the

interface cancel to some extent; a minimum in the smeared concentration profiles is nevertheless observed for $\psi > 1$ (Figure 1E).

The stark differences in the expected AFP concentration profiles for $\psi \ll 1$ and $\psi \gg 1$ can be exploited to determine whether AFP accumulation on ice is limited by adsorption or by diffusion. In particular, if AFP accumulation were diffusion-limited, i.e., $\psi > 1$, we would expect to observe a notable decrease in fluorescence intensity (below its bulk value) near the ice-water interface (for $t > \tau_{\mathrm{tr}}$ ~ seconds) with this decrease extending out over a distance that scales with the radius of the ice crystal, i.e., 10 μm. In contrast, we find that although AFPs continue to accumulate at the ice-water interface, the solution AFP concentration remains equal to its bulk value at all times (Figure 1C). These observations strongly suggest that AFP accumulation is limited by the intrinsic kinetics of adsorption, i.e., $\psi \ll 1$.

To obtain experimental estimates of ψ and k_{on}, we now make use of the fluorescence intensity, I_{int}, at the ice-water interface (corrected for the background intensity, as described in the refs. 3,4) which is proportional to the AFP surface concentration, n (Figure 1F). According to Equation 4 (and as detailed in the SI), the rate of interfacial AFP accumulation is approximately constant for $t > \tau_{\mathrm{tr}}$ and is given by: $\frac{\partial n}{\partial t} \approx \frac{DC_0}{R}\left(\frac{\psi}{1+\psi}\right)$. Correspondingly, the rate, $\mathcal{R}_I$, at which the normalized fluorescence intensity at the ice-water interface increases at early times (i.e., for small θ) is:

$$\mathcal{R}_I \equiv \frac{\partial}{\partial t}\left(\frac{I_{\mathrm{int}}}{I_{\mathrm{ref}}}\right) = \frac{\partial}{\partial t}\left(\frac{n}{n_{\mathrm{ref}}}\right) \approx \frac{DC_{\mathrm{o}}}{Rn_{\mathrm{ref}}}\left(\frac{\psi}{1+\psi}\right), \qquad (6)$$

where the reference intensity I_{ref} that is used to normalize I_{int} is chosen to be its long-time (or steady state) plateau value, $n_{\mathrm{ref}} = L_{\mathrm{ref}}^{-2}/N_{\mathrm{Avo}}$ is the corresponding AFP surface concentration,

and L_{ref} is the corresponding separation between bound AFPs. Thus, by combining our experimental estimate of $\mathcal{R}_I = 0.06\ \mathrm{s}^{-1}$ (inset of Figure 1F) and the experimental values of bulk AFP concentration $C_0 = 4.1$ μM and ice crystal radius $R = 11$ μm with our estimate of the AFP diffusion coefficient $D = 3.3 \times 10^{-11}\frac{\mathrm{m}^2}{\mathrm{s}}$ and an upper bound on the reference AFP surface concentration $n_{\mathrm{ref}} \lesssim 3 \times 10^{-8}\ \frac{\mathrm{mol}}{\mathrm{m}^2}$ (assuming $L_{\mathrm{ref}} \gtrsim 15$ nm, as was shown in ref. [5]), Equation 6 enables us to obtain: $\frac{\psi}{1+\psi} \approx \mathcal{R}_I\left(\frac{Rn_{\mathrm{ref}}}{DC_0}\right) \lesssim 0.037$, which then yields the experimental estimate, $\psi \lesssim 0.04$. This analysis conclusively shows that $\psi \ll 1$ and that AFP accumulation at the ice-water interface is limited by the kinetics of adsorption. Moreover, it highlights that for adsorption and diffusion rates to comparable (i.e., $\psi \approx 1$), the radius of the ice crystal would have to be larger than the threshold value, $R^* = 250$ μm.

To obtain an experimental estimate of the adsorption rate coefficient, we recognize that k_{on} is proportional to $\mathcal{R}_I$, and by following Equation 6, we obtain:

$$\mathcal{R}_I \approx \frac{DC_{\mathrm{o}}}{Rn_{\mathrm{ref}}}\left(\frac{\psi}{1+\psi}\right) = \frac{DC_{\mathrm{o}}}{Rn_{\mathrm{sat}}}\left(\frac{\psi}{1+\psi}\right)\left(\frac{n_{\mathrm{sat}}}{n_{\mathrm{ref}}}\right) = \frac{k_{\mathrm{on}}C_o}{1+\psi}\left(\frac{L_{\mathrm{ref}}}{L_{\mathrm{sat}}}\right)^2, \tag{7}$$

so that $k_{\mathrm{on}} \approx (L_{\mathrm{sat}}/L_{\mathrm{ref}})^2(1+\psi)\mathcal{R}_I/C_0$. We note that for $\psi \ll 1$, our estimate of k_{on} is relatively insensitive to the approximations made in estimating ψ. Moreover, as $L_{\mathrm{sat}} \leq L_{\mathrm{ref}}$, $k_{\mathrm{on}} \leq (1+\psi)\mathcal{R}_I/C_0$, and $(1+\psi)\mathcal{R}_I/C_0 = 0.016\ \mu\mathrm{M}^{-1}\mathrm{s}^{-1}$ represents an experimental upper bound for k_{on}. Another important consequence of the accumulation of AFPs being limited by adsorption is that AFP concentration near the ice-water interface, C_{surf}, remains equal to the bulk AFP concentration, C_0, at all times, and the time evolution of AFP surface concentration, $n(t)$, is decoupled from the spatiotemporal AFP concentration profile, $C(r,t)$. Thus, when adsorption follows Langmuir kinetics, i.e., $\mathcal{R}_{\mathrm{ads}} \approx k_{\mathrm{on}}C_0(n_{\mathrm{sat}} - n) - k_{\mathrm{off}}n$, we can integrate $\frac{dn(t)}{dt} = \mathcal{R}_{\mathrm{ads}}$

to obtain $\theta(t) = \frac{n(t)}{n_{\text{sat}}} = k_{\text{on}} C_0 \tau \left[1 - \exp\left(-\frac{t}{\tau}\right)\right]$, where the relaxation time, $\tau = (k_{\text{on}} C_0 + k_{\text{off}})^{-1}$. Because fluorescence intensity at the ice-water interface, I_{int}, is proportional to n, one can indeed fit the experimental $I_{\text{int}}(t)$ to an exponential function and estimate τ. Such estimates were obtained previously for different AFPs[4,5] over a range of bulk AFP concentration, C_0; the variation of τ^{-1} with C_0 was then fit to a straight line and the slope was reported as k_{on}. In particular, Drori *et al.*[3] reported a value of $k_{\text{on}} = 0.008 \pm 0.001\ \mu\text{M}^{-1}\text{s}^{-1}$ for AFPIII, which is consistent with our upper bound of $0.016\ \mu\text{M}^{-1}\text{s}^{-1}$.

Figure 2 presents the time evolution of the fluorescence intensity profiles for an antifreeze glycoprotein (AFGP$_{1\text{-}5}$) and a hyperactive AFP (*Tm*AFP). We also study AFGP$_{1\text{-}5}$ in the presence of borate, which interacts with the vicinal diols of the AFGP disaccharide moiety and lowers both the TH activity[23] of the AFGP as well as the rate of its adsorption to ice[4]. For all proteins, we

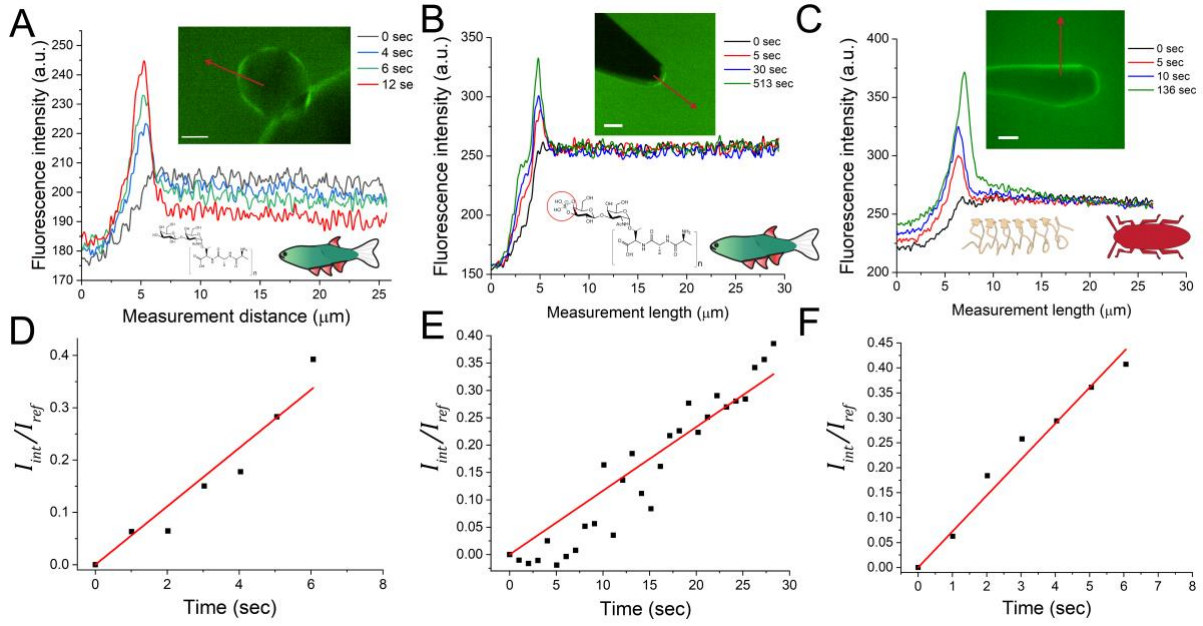

Figure 2: Spatio-temporal evolution of the fluorescence intensity for AFGP$_{1\text{-}5}$-FITC (A), AFGP$_{1\text{-}5}$-FITC with 0.3 M borate (B), and *Tm*AFP-GFP (C). Scale bar = 10 μm. For all proteins, the fluorescence intensity in the aqueous solution is independent of the distance from the ice-water interface at all times, whereas the peak intensity, which corresponds to the surface concentration of adsorbed proteins, increases monotonically with time. Time evolution of normalized fluorescence intensity at the ice-water interface is shown for AFGP$_{1\text{-}5}$-FITC (D), AFGP$_{1\text{-}5}$-FITC in 0.3 M borate (E), and *Tm*AFP-GFP (F).

observe that although the fluorescence intensity at the ice-water interface increases with time, the intensity in the aqueous solution does not fall below its bulk value. Thus, in contrast with the AFP concentration at the ice-water interface, which increases with time, the AFP concentration in the aqueous solution remains equal to its bulk value at all times. These observations were found to be independent of the bulk AFP concentration (Figures S1 and S2 present experiments with 8.4 and 3.1 μM AFPIII-QAE, respectively) and the crystal plane to which the proteins adsorb (Figure S3 presents experiments with *Tm*AFP adsorbing to the prism and basal planes of ice). The absence of a decrease in the solution AFP concentration below its bulk value over length scales comparable to the radius of the ice crystal strongly suggests that AFP accumulation at the ice-water interface is limited by adsorption and not by diffusion. Moreover, our estimates of ψ and k_{on}, included in Table 1 for all proteins studied here, confirm our key finding that the accumulation of diverse AFPs on ice is limited by the intrinsic kinetics of AFP adsorption. Although we do not focus on obtaining accurate estimates of k_{on} here, we note that our approximate estimates of k_{on} can be refined by performing experiments over a wide range of bulk AFP concentrations. Interestingly, our results suggest that the adsorption rate coefficient, k_{on}, of the flexible glycoprotein ($AFGP_{1\text{-}5}$), is quite similar to that of *Tm*AFP, which binds to ice via a relatively rigid beta-sheet. Moreover, a chemical modification of the $AFGP_{1\text{-}5}$ binding site (through the addition of borate) results in a substantial decrease in the corresponding k_{on}, highlighting the sensitivity of AFP adsorption kinetics to the chemistry of the binding site[4]. Finally, we note that our estimate of k_{on} for *Tm*AFP is roughly two orders of magnitude smaller than the prediction of Kamat et al.[18], which accounts for entropic barriers that stem from orientational restrictions faced by an AFP as it approaches the ice crystal; this difference suggests that additional barriers, which depend on the binding site chemistry, may be important in determining the overall adsorption kinetics.

Table 1: Experimental and calculated values for the adsorption of different AF(G)Ps to ice.

AF(G)P	C_0	R (μm)	$\mathcal{R}_I$ (s^{-1})	ψ	R^* (μm)	k_{on} ($\mu M^{-1}s^{-}$	k_{on}^{lit} ($\mu M^{-1}s^{-1}$)
AFPIII-QAE	4.1	11	0.06	0.039	285	0.015	0.008
$AFGP_{1-5}$	2.2	12	0.06	0.072	167	0.025	0.013
$AFGP_{1-5}$ + borate	8	10	0.01	0.003	3070	0.001	0.005
*Tm*AFP	2.9	9	0.07	0.052	172	0.025	-

CONCLUSIONS

In this article, we interrogate the relative importance of diffusion and adsorption in determining the rate of AFP accumulation on ice crystals by combining non-equilibrium fluorescence experiments with a reaction-diffusion model. We find that as diverse AFPs accumulate on ice crystals, which are roughly 10 microns in radius, their concentration in the aqueous solution is not depleted (relative to their bulk concentration), suggesting that the diffusion of AFPs is fast relative to their adsorption. By further analyzing the time-evolution of the surface concentration of adsorbed AFPs, we are able to quantify the relative rates of AFP adsorption and diffusion to be in the range of 0.003 to 0.07, leading us to conclude that the accumulation of diverse AFPs on ice is limited by the kinetics of AFP adsorption for ice crystals that are smaller than 150 μm in radius. Due to their small size, most insects do not have to contend with ice crystals that are larger than 100 μm. The internal ice crystals in fish, which are bipyramidal in shape[24], can be as large as 25 μm in radius and 100 μm in length[25]. Although larger crystals can form on the integument and gill epithelium of the fish[26], very large crystals with radii exceeding 150 μm have not been observed

inside fish, suggesting that in most biological contexts, the accumulation of AFPs on ice is not limited by diffusion, but by the kinetics of adsorption.

AUTHOR INFORMATION

Corresponding Authors

*Ran Drori, Department of Chemistry and Biochemistry, Yeshiva university, 245 Lexington Avenue, New York, NY 10016, USA, rdrori@yu.edu.

*Amish J. Patel, Department of Chemical and Biomolecular Engineering, University of Pennsylvania, Philadelphia PA 19104, USA, amish.patel@seas.upenn.edu.

ACKNOWLEDGMENT

The authors thank Prof. Peter Davies, Prof. Konrad Meister, and Prof. Arthur DeVries for kindly providing antifreeze protein samples. This material is based upon work supported by the U.S. Department of Energy, Office of Science, Office of Basic Energy Sciences, under Award Number DE-SC0021241. AJP gratefully acknowledges financial support from the Alfred P. Sloan Research Foundation (FG-2017-9406), the Camille & Henry Dreyfus Foundation (TC-19-033), and the National Science Foundation (grants CBET-1652646 and DMR-1720530). RD acknowledges the Donors of the American Chemical Society Petroleum Research Fund for support of this research (Grant number 60191-UNI5). IB acknowledges support from ERC (281595) and ISF (1308/21).

ASSOCIATED CONTENT

Supporting Information (PDF) includes additional experimental details, theoretical derivations that elaborate upon the implications of Equations 3 and 4 in certain limits, and Figures S1 – S3 containing supporting experimental results.

REFERENCES

(1) Raymond, J. A.; DeVries, A. L. Adsorption Inhibition as a Mechanism of Freezing Resistance in Polar Fishes. *Proc. Natl. Acad. Sci. U. S. A.* **1977**, *74* (6), 2589–2593.

(2) Bar Dolev, M.; Braslavsky, I.; Davies, P. L. Ice-Binding Proteins and Their Function. *Annu. Rev. Biochem.* **2016**, *85*, 515–542. https://doi.org/10.1146/annurev-biochem-060815-014546.

(3) Drori, R.; Celik, Y.; Davies, P. L.; Braslavsky, I. Ice-Binding Proteins That Accumulate on Different Ice Crystal Planes Produce Distinct Thermal Hysteresis Dynamics. *J. R. Soc. Interface* **2014**, *11* (98), 20140526. https://doi.org/10.1098/rsif.2014.0526.

(4) Meister, K.; DeVries, A. L.; Bakker, H. J.; Drori, R. Antifreeze Glycoproteins Bind Irreversibly to Ice. *J. Am. Chem. Soc.* **2018**, *140*, jacs.8b04966. https://doi.org/10.1021/jacs.8b04966.

(5) Drori, R.; Davies, P. L.; Braslavsky, I. Experimental Correlation between Thermal Hysteresis Activity and the Distance between Antifreeze Proteins on an Ice Surface. *RSC Adv.* **2014**.

(6) Drori, R.; Davies, P. L.; Braslavsky, I. When Are Antifreeze Proteins in Solution Essential for Ice Growth Inhibition? *Langmuir* **2015**, *31* (21), 5805–5811. https://doi.org/10.1021/acs.langmuir.5b00345.

(7) Pertaya, N.; Marshall, C. B.; DiPrinzio, C. L.; Wilen, L.; Thomson, E. S.; Wettlaufer, J. S.; Davies, P. L.; Braslavsky, I. Fluorescence Microscopy Evidence for Quasi-Permanent Attachment of Antifreeze Proteins to Ice Surfaces. *Biophys. J.* **2007**, *92* (10), 3663–3673. https://doi.org/10.1529/biophysj.106.096297.

(8) Haleva, L.; Celik, Y.; Bar-Dolev, M.; Pertaya-Braun, N.; Kaner, A.; Davies, P. L.;

Braslavsky, I. Microfluidic Cold-Finger Device for the Investigation of Ice-Binding Proteins. *Biophys J* **2016**, *111* (6), 1143–1150. https://doi.org/10.1016/j.bpj.2016.08.003.

(9) Celik, Y.; Drori, R.; Pertaya-Braun, N.; Altan, A.; Barton, T.; Bar-Dolev, M.; Groisman, A.; Davies, P. L.; Braslavsky, I. Microfluidic Experiments Reveal That Antifreeze Proteins Bound to Ice Crystals Suffice to Prevent Their Growth. *Proc. Natl. Acad. Sci. U. S. A.* **2013**, *110* (4), 1309–1314. https://doi.org/10.1073/pnas.1213603110.

(10) Tas, R. P.; Hendrix Marco M. R; Voets, I. K. Nanoscopy of Single Antifreeze Proteins Reveals That Reversible Ice Binding Is Sufficient for Ice Recrystallization Inhibition but Not Thermal Hysteresis. *Proc Natl Acad Sci U S A* **2023**, *120*, 1–8. https://doi.org/https://doi.org/10.1073/pnas.2212456120.

(11) Bar-Dolev, M.; Celik, Y.; Wettlaufer, J. S.; Davies, P. L.; Braslavsky, I. New Insights into Ice Growth and Melting Modifications by Antifreeze Proteins. *J. R. Soc. Interface* **2012**, *9* (77), 3249–3259. https://doi.org/10.1098/rsif.2012.0388.

(12) Scotter, A. J.; Marshall, C. B.; Graham, L. a; Gilbert, J. a; Garnham, C. P.; Davies, P. L. The Basis for Hyperactivity of Antifreeze Proteins. *Cryobiology* **2006**, *53* (2), 229–239. https://doi.org/10.1016/j.cryobiol.2006.06.006.

(13) DeVries, A. L. The Role of Antifreeze Glycopeptides and Peptides in the Freezing Avoidance of Antarctic Fishes. *Comp. Biochem. Physiol. -- Part B Biochem.* **1988**, *90* (3), 611–621. https://doi.org/10.1016/0305-0491(88)90302-1.

(14) Xiao, N.; Hanada, Y.; Seki, H.; Kondo, H.; Tsuda, S.; Hoshino, T. Annealing Condition Influences Thermal Hysteresis of Fungal Type Ice-Binding Proteins. *Cryobiology* **2014**, *68* (1), 159–161. https://doi.org/10.1016/j.cryobiol.2013.10.008.

(15) Takamichi, M.; Nishimiya, Y.; Miura, A.; Tsuda, S. Effect of Annealing Time of an Ice

Crystal on the Activity of Type III Antifreeze Protein. *FEBS J.* **2007**, *274* (24), 6469–6476. https://doi.org/10.1111/j.1742-4658.2007.06164.x.

(16) Knight, C. a.; DeVries, a. L. Ice Growth in Supercooled Solutions of a Biological "Antifreeze", AFGP 1-5: An Explanation in Terms of Adsorption Rate for the Concentration Dependence of the Freezing Point. *Phys. Chem. Chem. Phys.* **2009**, *11* (27), 5749–5761. https://doi.org/10.1039/b821256b.

(17) Hudait, A.; Moberg, D. R.; Qiu, Y.; Odendahl, N.; Paesani, F.; Molinero, V. Preordering of Water Is Not Needed for Ice Recognition by Hyperactive Antifreeze Proteins. *Proc. Natl. Acad. Sci.* **2018**, 201806996. https://doi.org/10.1073/pnas.1806996115.

(18) Kamat, K.; Naullage, P. M.; Molinero, V.; Peters, B. Diffusion Attachment Model for Long Helical Antifreeze Proteins to Ice. *Biomacromolecules* **2022**, *23* (2), 513–519. https://doi.org/10.1021/acs.biomac.1c01247.

(19) Kamat, K.; Naullage, P. M.; Molinero, V.; Peters, B. Oriented Attachment Kinetics for Rod-like Particles at a Flat Surface: Buffon's Needle at the Nanoscale. *J. Chem. Phys.* **2022**, *157* (21). https://doi.org/10.1063/5.0124531.

(20) Berger, T.; Meister, K.; DeVries, A. L.; Eves, R.; Davies, P. L.; Drori, R. Synergy between Antifreeze Proteins Is Driven by Complementary Ice-Binding. *J Am Chem Soc* **2019**, *141* (48), 19144–19150. https://doi.org/10.1021/jacs.9b10905.

(21) Miura, T.; Seki, K. Diffusion Influenced Adsorption Kinetics. *J. Phys. Chem. B* **2015**, *119* (34), 10954–10961. https://doi.org/10.1021/acs.jpcb.5b00580.

(22) Dehaoui, A.; Issenmann, B.; Caupin, F. Viscosity of Deeply Supercooled Water and Its Coupling to Molecular Diffusion. *Proc. Natl. Acad. Sci. U. S. A.* **2015**, *112* (39), 12020–12025. https://doi.org/10.1073/pnas.1508996112.

(23) Ebbinghaus, S.; Meister, K.; Born, B.; Devries, A. L.; Gruebele, M.; Havenith, M. Antifreeze Glycoprotein Activity Correlates with Long-Range Protein-Water Dynamics. *J. Am. Chem. Soc.* **2010**, *132* (35), 12210–12211. https://doi.org/10.1021/ja1051632.

(24) Deng, J.; Apfelbaum, E.; Drori, R. Ice Growth Acceleration by Antifreeze Proteins Leads to Higher Thermal Hysteresis Activity. *J. Phys. Chem. B* **2020**, *124* (49), 11081–11088. https://doi.org/10.1021/acs.jpcb.0c08119.

(25) Cziko, P. A.; DeVries, A. L.; Evans, C. W.; Cheng, C.-H. C. Antifreeze Protein-Induced Superheating of Ice inside Antarctic Notothenioid Fishes Inhibits Melting during Summer Warming. *Proc. Natl. Acad. Sci.* **2014**, *111* (40), 14583–14588. https://doi.org/10.1073/pnas.1410256111.

(26) Evans, C. W.; Gubala, V.; Nooney, R.; Williams, D. E.; Brimble, M. A.; Devries, A. L. How Do Antarctic Notothenioid Fishes Cope with Internal Ice? A Novel Function for Antifreeze Glycoproteins. *Antarct. Sci.* **2010**, *23* (1), 57–64. https://doi.org/10.1017/S0954102010000635.